A finite-element model for ocean acoustic propagation and scattering

Joseph E. Murphy
University of New Orleans, New Orleans, Louisiana 70128

Stanley A. Chin-Bing
Naval Ocean Research and Development Activity, Stennis Space Center, Mississippi 39529

(Received 2 December 1988; accepted for publication 22 June 1989)

The finite-element technique has the potential to provide a very accurate treatment of the physics of acoustic-wave propagation in inhomogeneous media. This article describes the development of a finite-element model for acoustic propagation in complex ocean environments and its validation. The computational model can handle range and depth dependence in both sound speed and density, as well as rapid variations in bottom topography.

PACS numbers: 43.30.Bp, 43.30.Hw

INTRODUCTION

There are many underwater acoustic propagation models currently in use in the scientific community, each of which has its own particular advantages and disadvantages. The need for more accurate models, particularly for applications at low frequencies where there can be significant boundary penetration, is growing. It is essential to give a more accurate treatment of the physics of acoustic/elastic-wave propagation. This, in turn, means that the computational models must include the effects of depth- and range-dependent sound speeds, bottom topography, and range-dependent shear in ocean sediments. The finite-element method has the potential to provide a very accurate treatment of the physics of wave propagation in such complex ocean environments.

The use of finite-element techniques to model acoustic waves is not new. Kalinowski has provided an excellent summary of the work of many authors, including his own, on the application of finite elements to various acoustic problems.[1] Earlier work has demonstrated that finite elements can be used to describe the effect of bottom shear on propagation over distances of a few wavelengths. A judicious blending of finite elements and the boundary integral method has been used to study sound–structure interactions for submerged bodies. Kuo and co-workers have used the finite-element method to model the time domain pulse propagation observed in laboratory scale models.[2] The two-dimensional finite-difference model of Stephen is similar in that it models pulse propagation and includes the effect of shear in the ocean bottom.[3] These models are well suited to study various types of geophysical phenomena in the time domain. Goldstein *et al.* have studied accelerated convergence methods for iterative numerical solution techniques applicable to the large systems of equations associated with finite-element models.[4] These iterative techniques are especially important when one deals with numerical solutions of elliptic equations that require large quantities of computer memory.

This article describes a finite-element ocean acoustic model (FOAM) which, in its present form, can very accurately model propagation over several kilometers. It handles depth- and range-dependent sound speed, density, and almost arbitrary variations in bottom topography. It does not yet include shear effects, and compared to some other types of models such as the parabolic equation (PE) model, it is computationally slow. However, unlike the one-way PE models and most normal-mode models, it is a full-wave solution, i.e., it includes backscatter and both the discrete modes and continuous spectra. There are no restrictions on angles of propagation. Unlike the time-domain models previously mentioned, which are often applied to seismic phenomena, ours is a frequency-domain model designed primarily for transmission loss studies.

In Sec. I, the finite-element mesh utilized in the model is discussed, as is the particular form of the basis or interpolation functions. Then, in Sec. II, the development of the finite-element equations is sketched, followed by the numerical solution technique in Sec. III. Two of the ways in which the physics and the computer code were verified are described in Sec. IV. A brief summary of our results and conclusions, as well as future plans to continue the development of the model are given in Sec. V.

I. FINITE-ELEMENT MESH AND INTERPOLATION FUNCTIONS

In the application of the finite-element technique to solving partial differential equations, the differential equation, and its unknown solution are replaced by a system of algebraic equations in terms of the parameters defining an approximate solution. One partitions the domain of the problem into nonoverlapping *elements* and assumes a simple form for the approximate solution within each element. These local representations are then joined together by using the appropriate physical continuity conditions to provide a global solution. The partial differential equations and associated boundary conditions that arise in many science and engineering problems give matrix systems of equations which are sparse, banded, and often symmetric. Fortunate-

 0001-4966/89/101478-06$00.80

ly, that is the case, too, for the description of ocean acoustic-wave propagation. The reader unfamiliar with finite-element techniques may want to consult the excellent text by Reddy.[5]

Consider the typical problem of ocean acoustics suggested by Fig. 1. An acoustic source is placed somewhere in the water column. The sound speed, whether in the water or in the ocean bottom, may vary with both depth and range. The depth of the water–bottom interface may vary with range. The acoustic pressure is taken to vanish at the air–water interface. If the ocean bottom is assumed to be homogeneous beyond some maximum depth, and if the sound-speed profiles do not vary beyond some maximum range, then along the right and bottom sides of the domain to be modeled one needs to impose some kind of approximate boundary condition which does not reflect any energy back into the interior.

Although basis or interpolation functions can be constructed for many types of polygonal regions, the triangle is one of the most widely used finite elements. At present, the computer model FOAM makes use of linear Lagrange interpolation functions. For each finite element Ω^e that makes up the domain to be modeled, one must form a set of interpolation functions. The unknown solution will be expressed as a linear combination of these interpolation functions. In addition to vanishing outside the element Ω^e, these functions satisfy the following conditions:

$$\psi_i^{(e)}(z_j,r_j) = \delta_{ij}, \tag{1}$$

$$\sum_{i=1}^{3} \psi_i^{(e)}(z,r) = 1, \tag{2}$$

where r_i,z_i is the location of the ith vertex of the element. Finite-element models generally make use of two node numbering schemes: a local one as used here, $i = 1, 2$, or 3, and a global one, $I = 1,2,\ldots,n$, where n is the total number of nodes in the mesh. Given the element number, one can map from the local node numbers to the global node numbers.

For triangular elements with linear interpolation functions, the ψ_i are given by

$$\psi_i^{(e)}(z,r) = (\alpha_i + \beta_i z + \gamma_i r)/2A_e, \tag{3}$$

where α_i, β_i, and γ_i are the constants

$$\alpha_i = z_j r_k - z_k r_j, \quad \beta_i = r_j - r_k, \quad \gamma_i = z_k - z_j. \tag{4}$$

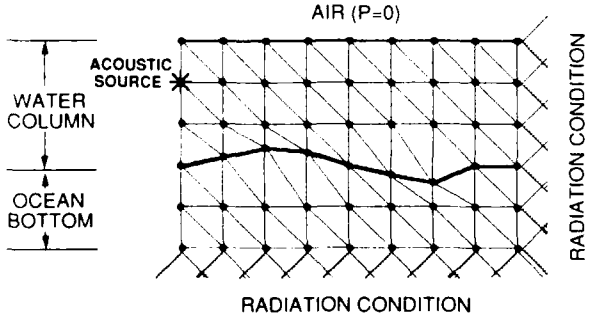

FIG. 1. Schematic drawing illustrating the finite-element mesh, boundary conditions, and nodes adjusted to follow the ocean bottom bathymetry.

In the above equations, $i \neq j \neq k$, and i, j, and k permute in a natural order. The constant A_e is the area of the triangle.

Integrals involving products of two or more interpolation functions can be simplified by the use of area coordinates L_i, where

$$L_i(z,r) = A_i/A_e = \psi_i(z,r). \tag{5}$$

Geometrically, A_i is the area of the triangle formed by the point (z,r) and nodes j and k. The following integration formula is quite useful for evaluating several of the required integrals:

$$\int (L_1)^m (L_2)^n (L_3)^p \, dA = \frac{m!n!p!}{(m+n+p+2)!} 2A_e, \tag{6}$$

where m, n, and p are arbitrary non-negative integers.

In our computer model, we have used triangular three-node elements, as previously discussed, so that the pressure within each element will be expressed as a linear combination of these interpolation functions:

$$P^{(e)}(z,r) = \sum_{j=1}^{3} P_j \psi_j^{(e)}(z,r). \tag{7}$$

Extensions to four-node, six-node, etc. triangles will allow more accurate representations of the pressure field since these require quadratic, cubic, and higher-order polynomial expressions for the interpolation functions.

II. THEORY

The time-harmonic complex pressure resulting from a point source of unit strength and angular frequency ω at position $\mathbf{r}_s$ in an inhomogeneous ocean is determined by the wave equation

$$\rho \nabla \cdot (\rho^{-1} \nabla P) + k^2 P = -\delta(\mathbf{r} - \mathbf{r}_s), \tag{8}$$

and appropriate boundary conditions. We will make the common assumption of an ocean environment axially symmetric about a vertical line passing through the source, so that in the above equation, $\rho = \rho(z,r)$ is the density, $k = k(z,r) = \omega/c(z,r)$ is the wavenumber and $c(z,r)$ is the sound speed. To allow for attenuation, the wavenumber can be given an imaginary part,

$$k = (\omega/c)(1 + i\eta\alpha), \tag{9}$$

where α is the attenuation of the medium in units of dB per wavelength and $\eta = (40\pi \log_{10} e)^{-1}$.

The finite-element technique will eventually yield a set of pressure values at the nodes of the grid as illustrated in Fig. 1. One of the key features of the method is the ability to use a grid of elements adapted to the specific problem. For example, if the density has a discontinuous jump in going across the water–bottom interface, the mesh would be formed so that the interface coincides with the boundaries of the appropriate interior elements.

A. Finite-element equations

One uses the wave equation within each element (and the interpolation functions defined for that element) to arrive at its contribution to the system of equations. Let us consider an element Ω^e that does not contain the source.

Multiply Eq. (8) by a test function V and integrate over the element Ω^e:

$$\int_{\Omega^e} \rho^{-1} \nabla v \cdot \nabla P r \, dA - \int_{\Omega^e} \rho^{-1} k^2 v P r \, dA - \int_{\Gamma^e} \rho^{-1} v \left(\frac{\partial P}{\partial n} \right) r \, dl = 0, \tag{10}$$

where the divergence theorem has been used to transform one of the integrals. The integrals are over the volume of the element Ω^e and around the boundary Γ^e of the element. Because of the assumption of axisymmetry, the solution and the test function are taken to depend upon z and r only. The volume differential is $d\tau = 2\pi r \, dr \, dz = 2\pi r \, dA$, and a common factor of 2π has been canceled everywhere. The partial derivative in the last integrand is with respect to the normal to the element's boundary.

Take the test function v to be equal to one of the interpolation functions, say, ψ_i, and in the first two integrals express the pressure within the element in the form

$$P = \sum_{j=1}^{3} P_j \psi_j^{(e)}, \tag{11}$$

Eq. (10) becomes,

$$\sum_{j=1}^{3} \left(\int_{\Omega^e} \rho^{-1} \nabla \psi_i^{(e)} \cdot \nabla \psi_j^{(e)} r \, dA - \int_{\Omega^e} \rho^{-1} k^2 \psi_i^{(e)} \psi_j^{(e)} r \, dA \right) P_j - \int_{\Gamma^e} \rho^{-1} \psi_i^{(e)} \left(\frac{\partial P}{\partial n} \right) r \, dl = 0. \tag{12}$$

If the density ρ and wavenumber k are treated as constants within each element, the first and second integrals in Eq. (12) can be evaluated exactly. They are proportional to the following two integrals:

$$K_{ij}^{(e)} = \int \nabla \psi_i^{(e)} \cdot \nabla \psi_j^{(e)} r \, dA, \tag{13}$$

$$M_{ij}^{(e)} = \int \psi_i^{(e)} \cdot \psi_j^{(e)} r \, dA. \tag{14}$$

The second of these can be evaluated using the substitution

$$r = \sum_{k=1}^{3} r_k \psi_k \tag{15}$$

and then the integration formula given above in Eq. (6). Note that both $K_{ij}^{(e)}$ and $M_{ij}^{(e)}$ are symmetric matrices. They are usually referred to as stiffness and mass matrices, respectively.

B. Boundary integrals and boundary conditions

For those elements that are in the interior, the boundary integral is not zero, but its contributions to the global system of equations will exactly cancel with like terms coming from neighboring elements. One only need recall that the term $\rho^{-1} \partial P / \partial n$ is proportional to particle displacement normal to the boundary and it must be continuous across the boundary. For the case where the element has one or two of its sides on an actual boundary of the FE model, one of three possible boundary conditions are allowed: (1) Neumann boundary condition, $\partial P / \partial n = 0$, (2) Dirichlet boundary condition, $P = 0$, or (3) radiating boundary condition. The first two conditions are treated exactly in the computer model using standard finite-element techniques. In the first case, the boundary integral is zero; so the first two integrals discussed are the only ones that contribute anything. In the second case, the equations involving the nodes for which $P = 0$ are simply replaced with $P_i = 0$. The third can only be treated approximately and requires considerably more work.

The radiating boundary condition means that waves should pass through the boundary without reflection. Ideally, one imposes a radiation condition infinitely far from the source. Usually, in a computer model one must use an approximate radiation condition on a finite boundary. At present, in FOAM, this can be treated approximately by one of two boundary conditions—a narrow-angle radiation boundary condition or a wide-angle radiation boundary condition. These are both described below. The narrow-angle radiation condition, so-called because it is valid for plane waves incident on the boundary within a small angular interval about the normal, is equivalent to a damping condition used earlier by Kalinowski.[1] It is given by the equation

$$\frac{\partial P}{\partial n} = ikP. \tag{16}$$

The wide-angle radiation condition that we have developed is useful for a somewhat wider interval about the normal direction and is actually a kind of PE used as a boundary condition:

$$\frac{\partial P}{\partial n} = ikP + \left(\frac{i}{2k} \right) \frac{\partial^2 P}{\partial s^2}, \tag{17}$$

where the derivatives $\partial^2 / \partial s^2$ are taken tangent to the boundary. A comparison that shows the advantage of the second radiating boundary condition over the first is illustrated in Fig. 2(a), where the effective reflection coefficients for these two boundary conditions are plotted. The percent of incident energy reflected is shown in Fig. 2(b). One can conclude that the wide-angle radiation condition allows a higher incident angle to be reached before the solution is seriously contaminated by false reflections.

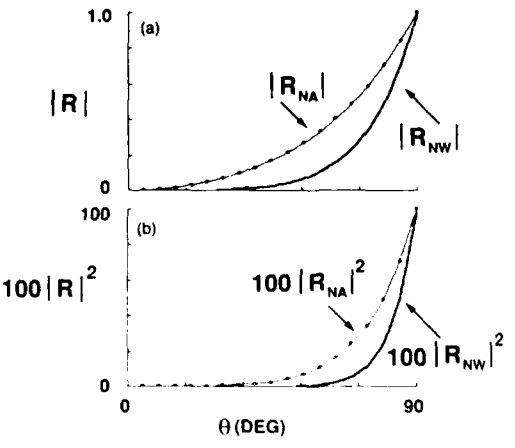

FIG. 2. Comparisons of (a) reflection coefficients and (b) intensities as a function of incident angle for the narrow-angle (NA) and wide-angle (WA) radiation conditions.

Upon substituting these approximate radiating boundary conditions into Eq. (12) in the last term, one finds that their contributions can be written in terms of one or both of the integrals:

$$B_{ij}^{(e)} = \int \left(\frac{\partial \psi_i^{(e)}}{\partial s}\right)\left(\frac{\partial \psi_j^{(e)}}{\partial s}\right) r\, dl, \tag{18}$$

$$C_{ij}^{(e)} = \int \psi_i^{(e)} \cdot \psi_j^{(e)} r\, dl. \tag{19}$$

Both are symmetric matrices, and the global equations resulting from either of these boundary conditions are still symmetric, an important feature for the solution technique. A small amount of attenuation can be introduced near any radiating boundaries to further extinguish unwanted reflections.

Once the contributions of the various elements is determined, the global system of equations is formed by mapping the local node numbers onto the global node numbers, giving rise to the *global pressure vector* **P**, and combining all of the subsystems into a single global system of equations. The source contribution appears as a single entry in the *global force vector* **GF**, and the stiffness, mass, and boundary contributions finally yield a *global stiffness matrix* **GSTIFF**. One then must solve the system

$$\mathbf{GSTIFF} \cdot \mathbf{P} = \mathbf{GF}, \tag{20}$$

where **P** and **GF** are n-dimensional vectors, and **GSTIFF** is the $n \times n$ system matrix; here, n is the total number of pressure nodes in the finite element mesh.

III. NUMERICAL SOLUTION

The global stiffness matrix is a complex, symmetric matrix that can be factored in the following form[6]:

$$\mathbf{GSTIFF} = \mathbf{U}^{\mathrm{T}}\mathbf{D}\mathbf{U}, \tag{21}$$

where **U** is an upper triangular $n \times n$ matrix with ones along its diagonal, and **D** is an $n \times n$ diagonal matrix. The most time consuming part of the calculations is the factorization of **GSTIFF**. One can generate the U_{ij} and D_{jj} in a column-wise fashion by using the recurrence equations given below for $j = 2,3,\ldots,n$:

$$U_{ij} = \left(\frac{1}{D_{ii}}\right)\left(A_{ij} - \sum_{k=1}^{j-1} D_{kk} U_{ki} U_{kj}\right), \quad 1 < i < j, \tag{22}$$

$$D_{jj} = A_{jj} - \sum_{k=1}^{j-1} D_{kk} U_{kj}^2, \quad 1 < i = j. \tag{23}$$

Afterwards, the complex pressure is obtained in three steps. In the first step, one solves for the complex vector **Z** in the lower triangular system,

$$\mathbf{U}^{\mathrm{T}}\mathbf{Z} = \mathbf{GF}. \tag{24}$$

Since $\mathbf{U}^{\mathrm{T}}$ is a lower triangular matrix, the Z_i can be calculated in a series of forward substitutions:

$$Z_i = GF_i - \sum_{j=1}^{i-1} U_{ji} GF_j, \quad i > 1. \tag{25}$$

The second step consists of solving for the complex vector **Y** defined by the diagonal system

$$\mathbf{DY} = \mathbf{Z}. \tag{26}$$

Since **D** is a diagonal matrix, the Y_i are simply equal to Z_i/D_i. Finally, the desired pressure vector results from solving the upper triangular system:

$$\mathbf{UP} = \mathbf{Y}. \tag{27}$$

The elements of **P** are found by a series of back substitutions:

$$P_i = Y_i - \sum_{j=i+1}^{n} U_{ij} P_j, \quad i < n. \tag{28}$$

The computer model uses a banded version of a factorization algorithm to take full advantage of the banded nature of **GSTIFF** and **U** to minimize the storage requirements.[7]

IV. MODEL VERIFICATION

In addition to solving a number of boundary value problems with boundary conditions selected to yield solutions with particular types of symmetries, the model has been used to solve two problems more familiar to the underwater acoustics community, i.e., the Lloyd's mirror effect and an upslope wedge propagation benchmark problem recently discussed at Acoustical Society of America meetings.

A. Lloyd's mirror effect

As an early test of the accuracy of our FE model, the Lloyd's mirror effect was examined. This image-interference effect occurs in underwater acoustics when the acoustic source is near the sea surface and the sea surface is not very rough (i.e., the sea surface acts as a pressure-release surface). Then, an interference pattern in the sound field results from constructive and destructive interference between the direct and surface-reflected acoustic waves. There is an analytic solution[8] that was used as a baseline result against which the FOAM calculations could be compared. Figure 3 shows two contour plots of constant pressure at 2-dB intervals for an upper half-space of air and a lower half-space of

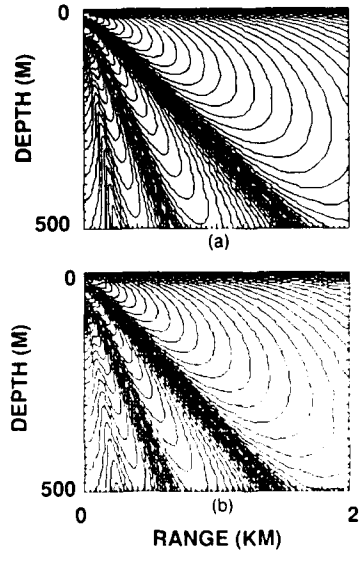

FIG. 3. Contour plots of the Lloyd's mirror effect computed by (a) an exact solution and (b) FOAM using the wide-angle radiation condition. Contours start at 0 dB and increase in intervals of 3 dB.

water with 0.5 dB per wavelength absorption. The 25-Hz cw source was placed 100 m below the surface. The familiar Lloyd's mirror beams[9] are quite evident. Unlike the analytic solution, our model must simulate the lower half-space using a bounded medium terminating with a radiation boundary condition. The results shown in Fig. 3(b) were obtained using the wide-angle radiation boundary condition on the bottom and right boundaries of our model, and compare favorably with the analytic solution [Fig. 3(a)] except near the radiating boundaries. Some low grazing angle reflections are evident along the bottom and right side as can be seen by comparing the two figures below.

Although this appears to be a very simple problem, i.e., a point source in a homogeneous half-space with a pressure release surface, it is one that cannot be done very well with most PE's since they cannot handle the steep beams, nor will they give correct results at very short ranges. It also provides a rather stringent test of the radiation boundary condition that we have developed for the bottom and far right boundaries of the computational model.

B. ASA benchmark problem

In 1987 at the 113th meeting of the Acoustical Society of America (ASA), a special session was devoted to numerical solutions of several types of benchmark problems.[10] One problem dealt with upslope propagation in a wedge-shaped underwater channel. A 25-Hz cw acoustic source was placed at a depth of 100 m below the surface of the water. The ocean bottom was initially 200 m deep and gradually decreased in depth at a 2.86-deg rise until it intersected the ocean surface at a range of 4.0 km. The density of the water was 1 g/cc and the sound speed was 1500 m/s. The wedge half-space had a density of 1.5 g/cc, a sound speed of 1700 m/s, and an attenuation of 0.5-dB/wavelength. In addition to the continuous spectra, the source excites three propagating modes that pass through their cutoff depths at ranges of approximately 813, 2088, and 3363 m.

A range-dependent coupled-mode model[11] was used as the benchmark result[12] against which other models were compared. Figure 4 shows a comparison of our FOAM results (solid curve) compared to the coupled-mode benchmark model results (broken curve). The transmission loss curves are almost indistinguishable. A contour plot showing transmission loss is given in Fig. 5. One can see the effect of mode dumping at the appropriate ranges. Both of these models are full-wave range-dependent models and can account for the backscatter and interference that comes from the wedge. Clearly, the finite-element results compare very favorably with the benchmark results. Because the many presenters at the benchmark session used a number of different computers and did not all give cpu times, we are not able to make a comparison of relative computational effort.

V. SUMMARY AND CONCLUSIONS

The development of a finite-element model for acoustic propagation in complex ocean environments, FOAM, has been described. Results of two tests used to verify the model, the Lloyd's mirror effect, and an upslope wedge propagation

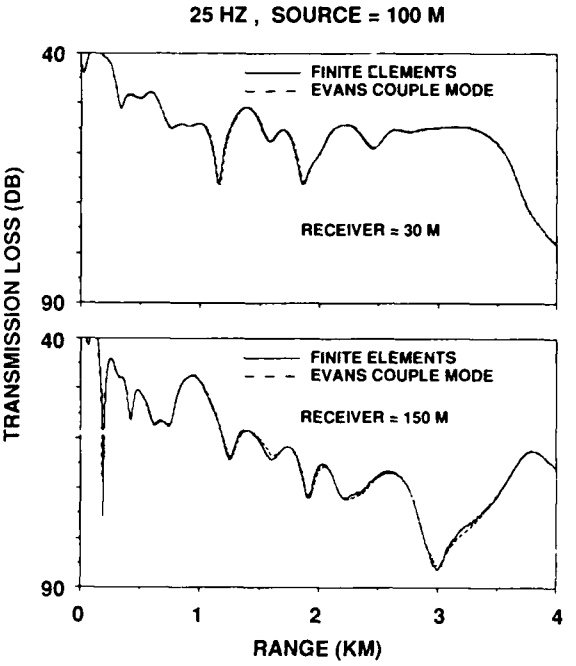

FIG. 4. Transmission loss plots (in dB) for the ASA benchmark wedge problem, comparing FOAM with the ASA benchmark solution obtained from the Evans' coupled mode model.

problem discussed extensively at recent ASA meetings have been shown. The transmission loss calculations using the finite-element model compare very favorably with the analytical and benchmark solutions. Because of its potential to provide a very complete treatment of propagation in complex ocean environments, we believe that it is important to continue its development, particularly to include shear effects in the ocean bottom and to extend it to three-dimensional environments, while at the same time working to improve its computational efficiency and to remove its current restriction to short ranges. The latter is principally a computer memory problem, not a restriction of the finite-element technique itself.

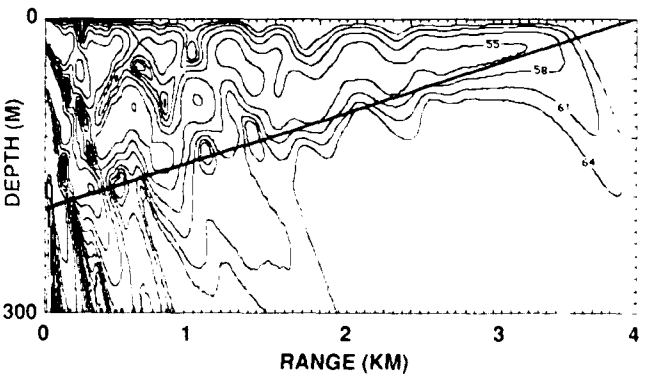

FIG. 5. Contour plot (in dB) from FOAM for the ASA benchmark wedge problem.

ACKNOWLEDGMENTS

Part of this work was done while one of the authors (J.E.M.) was on sabbatical leave from the University of New Orleans and held visiting appointments at the Institute for Naval Oceanography (INO) and the Naval Ocean Research and Development Activity (NORDA), both located at the John C. Stennis Space Center. We are both grateful to INO for the use of their computer facilities. We thank Dr. Finn Jensen of SACLANT for providing us with his numerical results using Dr. Richard Evans' COUPLE model. This work was supported by the Office of Naval Research and NORDA, NORDA contribution No. JA 221:014:89. Approved for public release; distribution is unlimited.

[1]F. R. DiNapoli and D. L. Deavenport, "Numerical Models of Underwater Acoustic Propagation," in *Ocean Acoustics*, edited by J. A. DeSanto (Springer-Verlag, Berlin, 1979). Chapter 3 contains a synopsis by A. J. Kalinowski on the applicability of finite-element techniques to acoustic propagation problems, pp. 142–154. See, also, the references contained therein.

[2]J. T. Kuo, "The influence of the elasticity of the ocean bottom on wave propagation," in *Computational Acoustics: Wave Propagation*, edited by D. Lee, R. L. Sternberg, and M. H. Schultz (Elsevier, New York, 1988), pp. 199–223; Y. C. Teng and J. T. Kuo, "A finite element algorithm for solving the transient problem in a fluid-solid coupled medium," in *Computational Acoustics: Wave Propagation*, edited by D. Lee, R. L. Sternberg, and M. H. Schultz (Elsevier, New York, 1988), pp. 239–257; J. T. Kuo, Y. C. Teng, P. Pecholcs, and J. Blair, "A note on the influence of the elasticity on wave propagation in an acoustic/elastic coupled medium," Comput. Math. Appl. **11**, 887–896 (1985).

[3]R. A. Stephen, "A comparison of finite difference and reflectivity seismograms for marine models," Geophys. J. R. Astron. Soc. **72** 39–58 (1983); R. A. Stephen, "Finite difference seismograms for laterally varying marine models," Geophys. J. R. Astron. Soc. **79**, 184–198 (1984); M. E. Dougherty and R. A. Stephen, "Geoacoustic scattering from seafloor features in the ROSE area," J. Acoust. Soc. Am. **82**, 238–256 (1987).

[4]C. I. Goldstein, "Finite element methods applied to nearly one-way wave propagation," J. Comput. Phys. **64**, 56–81 (1986); A. Bayliss, C. I. Goldstein, and E. Turkel, "An iterative method for the Helmholtz equation," J. Comput. Phys. **49**, 443–457 (1983); A. Bayliss, C. I. Goldstein, and E. Turkel, "The numerical solution of the Helmholtz equation for wave propagation problems in underwater acoustics," Comput. Math. Appl. **11**, 655–665 (1985).

[5]J. N. Reddy, *An Introduction to the Finite Element Method* (McGraw-Hill, New York, 1984).

[6]O. Axelsson, and V. A. Barker, *Finite Element Solution of Boundary Value Problems* (Academic, New York, 1984), pp. 279–287.

[7]W. Weaver, Jr. and P. R. Johnson, *Finite Elements for Structural Analysis* (Prentice-Hall, Englewood Cliffs, NJ, 1984), Appendix C.

[8]C. B. Officer, *Introduction to the Theory of Sound Transmission* (McGraw-Hill, New York, 1958), pp. 110–115.

[9]H. Schmidt and F. B. Jensen, "Efficient numerical solution technique for wave propagation in horizontally stratified environments," in *Computational Ocean Acoustics*, edited by M. H. Schultz and D. Lee (Pergamon, New York, 1985), pp. 706–708.

[10]L. B. Felsen, "Numerical solutions of two benchmark problems," J. Acoust. Soc. Am. Suppl. 1 **81**, S39 (1987).

[11]R. B. Evans, "A coupled mode solution for acoustic propagation in a waveguide with stepwise depth variations of a penetrable bottom," J. Acoust. Soc. Am. **74**, 188–194 (1983).

[12]F. B. Jensen, "Coupled mode and parabolic equation solutions," J. Acoust. Soc. Am. Suppl. 1 **81**, S40 (1987).

REPORT DOCUMENTATION PAGE

Form Approved
OMB No. 0704-0188

1. Agency Use Only *(Leave blank).*	2. Report Date.	3. Report Type and Dates Covered.
	1989	Journal Article

4. Title and Subtitle.
A finite-element model for ocean acoustic propagation and scattering

5. Funding Numbers.
Program Element No. 61153N
Project No. 03205
Task No. 330
Accession No. DN257033

6. Author(s).
Joseph E. Murphy and Stanley A. Chin-Bing

7. Performing Organization Name(s) and Address(es).
Naval Oceanographic and Atmospheric Research Laboratory*
Stennis Space Center, MS 39529-5004

8. Performing Organization Report Number.
JA 221:014:89

9. Sponsoring/Monitoring Agency Name(s) and Address(es).
Naval Oceanographic and Atmospheric Research Laboratory*
Stennis Space Center, MS 39529-5004

10. Sponsoring/Monitoring Agency Report Number.
JA 221:014:89

11. Supplementary Notes.
*Formerly Naval Ocean Research and Development Activity

12a. Distribution/Availability Statement.
Approved for public release; distribution is unlimited.

12b. Distribution Code.

13. Abstract *(Maximum 200 words).*
The finite-element technique has the potential to provide a very accurate treatment of the physics of acoustic-wave propagation in inhomogeneous media. This article describes the development of a finite-element model for acoustic propagation in complex ocean environments and its validation. The computational model can handle range and depth dependence in both sound speed and density, as well as rapid variations in bottom topography.

14. Subject Terms.
(U) Acoustic Waves; (U) Elastic Waves; (U) Seismic Waves

15. Number of Pages.
6

16. Price Code.

17. Security Classification of Report.	18. Security Classification of This Page.	19. Security Classification of Abstract.	20. Limitation of Abstract.
Unclassified	Unclassified	Unclassified	SAR

NSN 7540-01-280-5500

Standard Form 298 (Rev 2-89)
Prescribed by ANSI Std Z39-18
298-102